Transient analysis of organic electrophosphorescence. II. Transient analysis of triplet-triplet annihilation

Baldo, Marc.A.
Center for Photonics and Optoelectronic Materials (POEM), Department of Electrical Engineering and the Princeton Materials Institute, Princeton University

Adachi, Chihaya
Center for Photonics and Optoelectronic Materials (POEM), Department of Electrical Engineering and the Princeton Materials Institute, Princeton University

Forrest, Stephen R.
Center for Photonics and Optoelectronic Materials (POEM), Department of Electrical Engineering and the Princeton Materials Institute, Princeton University

出版情報：Physical Review B. 62 (16), pp.10967-10977, 2000-10-15. The American Physical Society
バージョン：
権利関係：? The American Physical Society

Transient analysis of organic electrophosphorescence. II. Transient analysis of triplet-triplet annihilation

M. A. Baldo, C. Adachi, and S. R. Forrest
Center for Photonics and Optoelectronic Materials (POEM), Department of Electrical Engineering and the Princeton Materials Institute, Princeton University, Princeton, New Jersey 08544

(Received 3 January 2000; revised manuscript received 10 May 2000)

In the preceding paper, Paper I [Phys. Rev. B **62**, 10 958 (2000)], we studied the formation and diffusion of excitons in several phosphorescent guest-host molecular organic systems. In this paper, we demonstrate that the observed decrease in electrophosphorescent intensity in organic light-emitting devices at high current densities [M. A. Baldo *et al.*, Nature **395**, 151 (1998)] is principally due to triplet-triplet annihilation. Using parameters extracted from transient phosphorescent decays, we model the quantum efficiency versus current characteristics of electrophosphorescent devices. It is found that the increase in luminance observed for phosphors with short excited-state lifetimes is due primarily to reduced triplet-triplet annihilation. We also derive an expression for a limiting current density (J_0) above which triplet-triplet annihilation dominates. The expression for J_0 allows us to establish the criteria for identifying useful phosphors and to assist in the optimized design of electrophosphorescent molecules and device structures.

I. INTRODUCTION

The successful application[1–3] of phosphorescent molecules in generating efficient organic electroluminescence has facilitated a greater understanding of the physics of organic materials[4] and has also enabled the fabrication of organic light-emitting devices (OLED's) with remarkably high efficiencies.[3] Both of these attributes are a result of the ability of phosphors to emit light from the relaxation of triplet excitons formed by electron-hole combination after electrical injection of charge carriers.[1,5] Emission from a triplet state does not conserve spin; hence phosphorescence is a slower process than the spin-conserving singlet transitions responsible for fluorescence. But since approximately three triplet excitons are formed for every singlet,[4] without phosphorescent materials the bulk of excitons in an electroluminescent device is difficult to observe or study, and device internal electroluminescent quantum efficiency is limited to 25% or less.

In the first part of this work (Paper I), we discussed the influence of the host in phosphorescent guest-host organic systems.[6] In this part, we concentrate on the processes occurring when the excitons are localized on the guest molecules. One pronounced characteristic of electrophosphorescence is a roll-off in efficiency at high current densities.[1–3] In previous work, it has been noted that the onset of this roll-off occurs at increasing current densities as the transient phosphorescent lifetime is decreased.[3] Hence, the phosphor *fac* tris-(2-phenylpyridine) iridium [$Ir(ppy)_3$], with a ~500-ns excited-state lifetime,[3] has a significantly higher quantum efficiency at typical operating current densities of $J \sim 1$ mA/cm^2 than does 2,3,7,8,12,13,17,18-octaethylporphine platinum (PtOEP), with a lifetime[1] of ~30 μs. A possible explanation is that long transient lifetimes increase the likelihood for saturation of phosphorescent sites. Thus, devices incorporating a conductive organic host material doped with $Ir(ppy)_3$ saturate at higher current densities than similar PtOEP-doped devices. Indeed, this is confirmed by emission from the host molecules in PtOEP-doped devices at high current densities (~100 mA/cm^2) and the relative absence of such emissions in $Ir(ppy)_3$-doped devices. However, the onset of the efficiency roll-off [~1 mA/cm^2 for PtOEP and ~100 mA/cm^2 for $Ir(ppy)_3$] occurs at much lower current density than is required to fully saturate phosphorescent sites[3] with a density of $\sim 10^{19}$ cm^{-3}. We would also expect that saturation of the luminescent sites would lead to an efficiency roll-off proportional to $1/J$, where J is the current density. But at the current densities of interest, the roll-off is much more gradual. Thus, saturation alone cannot explain the observed behavior. Rather, we show that the observations are consistent with triplet-triplet (T-T) annihilation dominating electrophosphorescence until relatively high current densities. From our model of T-T dynamics, we calculate an onset current density J_0 where biexcitonic triplet interactions become significant. This parameter can be used to quantify the relative merits of different phosphors employed in OLED's.

This paper is organized as follows: in Sec. II the theory of T-T annihilation is described, in Sec. III we discuss the fabrication of the electroluminescent devices used in this work, and in Sec. IV we study PtOEP and $Ir(ppy)_3$ doped into different host materials. In Sec. V we measure the rate of the competing process of triplet-charge carrier (polaron) annihilation. Finally, in Sec. VI, we discuss discrepancies between the results and our theoretical treatment, before concluding in Sec. VII.

II. THEORY

For simplicity of analysis we assume that only guest triplets participate in triplet-triplet annihilation and consider the following exothermic reactions:[7]

$$^3M^* + {}^3M^* \xrightarrow{k_{TT}^S} {}^1M^* + M, \tag{1}$$

$$^3M^* + {}^3M^* \xrightarrow{k_{TT}^T} {}^3M^* + M. \quad (2)$$

Here, $^3M^*$ represents the triplet excited state, $^1M^*$ the singlet excited state, and M the ground state of the molecule. The rate constants for the generation of singlets and triplets from a triplet-triplet reaction are k_{TT}^S and k_{TT}^T, respectively. In this work the phosphorescent guest molecules possess strong spin-orbit coupling; hence almost immediately following generation, singlets will cross to the triplet state, i.e.,

$$M + {}^1M^* \xrightarrow{\text{ISC}} M + {}^3M^*. \quad (3)$$

We define the total annihilation rate in Eqs. (1) and (2) as $k_{TT}[^3M^*]$. Since each annihilation event generates a single triplet exciton, the rate of triplet loss is $\frac{1}{2}k_{TT}[^3M^*]$. Hence to second order, the concentration of triplet excitons, $[^3M^*]$, is determined by the rate of triplet generation (proportional to current density J), and the rates of monoexcitonic and biexcitonic[8] triplet recombination, viz

$$\frac{d[^3M^*]}{dt} = -\frac{[^3M^*]}{\tau} - \frac{1}{2}k_{TT}[^3M^*]^2 + \frac{J}{qd}. \quad (4)$$

Here, q is the electron charge, d is the thickness of the exciton formation zone, and τ is the phosphorescent recombination lifetime.

The transient decay of $[^3M^*(t)]$ following an excitation pulse is

$$[^3M^*(t)] = \frac{[^3M^*(0)]}{\left(1 + [^3M^*(0)]\frac{k_{TT}\tau}{2}\right)e^{t/\tau} - [^3M^*(0)]\frac{k_{TT}\tau}{2}}. \quad (5)$$

Assuming that the luminescence intensity (L) is linearly proportional to the concentration of excited states, i.e., $L(t) \propto [^3M^*(t)]/\tau$, then the phosphorescent emission intensity is

$$L(t) = \frac{L(0)}{(1+K\tau)e^{t/\tau} - K\tau}, \quad (6)$$

where K is defined by

$$K = \tfrac{1}{2}k_{TT}[^3M^*(0)]. \quad (7)$$

The quantum efficiency of light emission (η) can also be calculated from the steady-state solution of Eq. (4) to give

$$\frac{\eta}{\eta_0} = \frac{J_0}{4J}\left(\sqrt{1 + 8\frac{J}{J_0}} - 1\right), \quad (8)$$

where η_0 is the quantum efficiency in the absence of T-T annihilation, and

$$J_0 = \frac{4qd}{k_{TT}\tau^2} \quad (9)$$

is the ''onset'' current density at $\eta = \eta_0/2$. For comparison, the current density required to excite every phosphorescent molecule (i.e., the onset of saturation) can also be calculated from Eq. (4). Ignoring the T-T annihilation term, we get

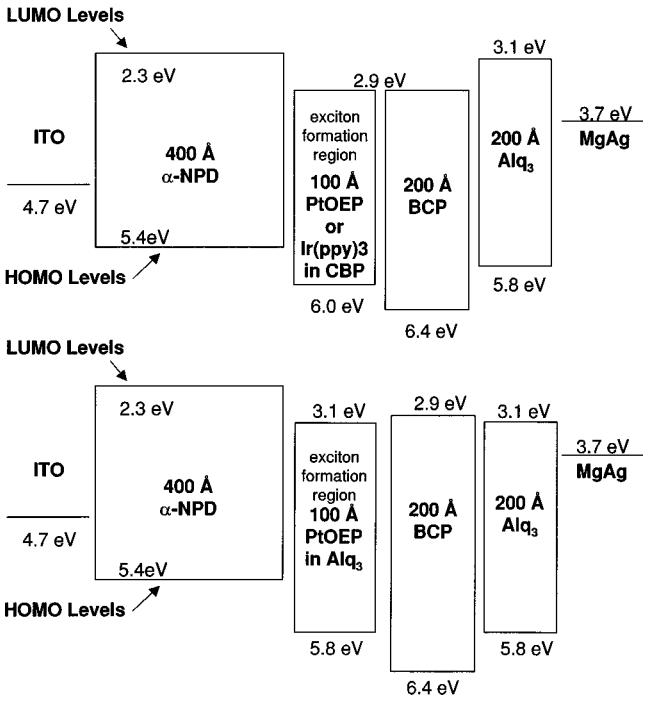

FIG. 1. Schematic cross sections of the electroluminescent devices fabricated in this work. To control the concentration of triplet excitons, the devices contain a narrow recombination and luminescent zone. After pulsed electrical excitation, transient phosphorescence was measured by a streak camera and fitted to Eq. (6). Proposed energy levels of the highest occupied molecular orbital (HOMO) and lowest unoccupied molecular orbital (LUMO) are shown for devices containing Alq_3 and CBP, the two luminescent host materials used in this work.

$$J_s = \frac{[M]qd}{\tau}, \quad (10)$$

where $[M]$ is the total concentration of phosphorescent molecules.

In the following section, we analyze triplet dynamics in five materials systems: PtOEP in 4,4′-*N*,*N*′-dicarbazole-biphenyl (CBP), where according to Paper I, triplets are formed primarily on PtOEP and the concentration of CBP triplets is minimal; PtOEP in tris-(8-hydroxyquinoline) aluminum (Alq_3), which exhibits Dexter energy transfer of triplets between species; $Ir(ppy)_3$ in CBP, where most triplets are formed directly on $Ir(ppy)_3$ but there may also be a significant population of triplets in the host; PtOEP in $Ir(ppy)_3$, which may exhibit Förster energy transfer of triplets from $Ir(ppy)_3$ to PtOEP, and finally a lanthanide complex, $Eu(TTA)_3$phen (TTA=thenoyltrifluoroacetone; phen=1, 10-phenanthroline) in CBP.

III. EXPERIMENTAL METHOD

The electrically pumped structures shown in Fig. 1 were fabricated to study transient lifetimes and T-T annihilation in different host and phosphorescent guest molecular combinations. The fabrication process follows procedures described[6] in Paper I.

The molecular structural formulas of most guest and host materials employed are shown in Fig. 1 of Paper I. Follow-

ing Paper I, the proposed energy-level diagrams[9] of the device structures employed are shown in Fig. 1 here, as inferred from direct measurement of the ionization potentials and optical energy gaps of the various molecular species.[6,9] In all devices, the thin bathocuproine (BCP) (2,9-dimethyl-4,7 diphenyl-1, 10-phenanthroline) layer acts to confine excitons within the formation zone adjacent to either the Alq_3/α-NPD (4,4′-bis[*N*-(1-napthyl)-Nphenylamino]biphenyl) or the CBP/BCP interface. It possesses a large energy gap ($\sim$3.5 eV), and the energy step between the highest occupied molecular orbital (HOMO) of the host materials and of BCP (shown in Fig. 1) prevents holes from diffusing into the undoped Alq_3 ETL. Measurements of film photoluminescence (PL) and OLED external quantum efficiency were performed following procedures discussed in Paper I.

IV. EXPERIMENTAL RESULTS AND ANALYSIS

In this section we study triplet-triplet annihilation in several different combinations of guest and host materials. In Sec. IV A we demonstrate the existence of T-T effects in a simple photoexcited system. Then in Secs. IV B–IV D we examine the effect of the triplet energy difference (ΔG) between the guest and host on the strength of the T-T mechanism. Using the results of Paper I, we find that good agreement with the simple T-T theory of Eq. (4) is found in systems where ΔG is greatest, and triplets are well confined to the guest phosphor. In Sec. IV E, we use $Ir(ppy)_3$ as the host material to enable rapid Förster transfer of triplets to the guest. Such a system not only confines triplets on the guest, but also exhibits[10] rapid ($\sim$100-ns) energy transfer to the guest. Finally, in Sec. IV F, we examine $Eu(TTA)_3$phen, where the emissive species is not a triplet, but where triplets nevertheless participate in the energy transfer.

A. Triplet-triplet annihilation

To observe T-T annihilation, a film of 4% PtOEP doped in CBP (4% PtOEP:CBP) was excited by the pulsed N_2 laser, generating singlet excitons on both the CBP and PtOEP molecules. The relatively high-energy CBP singlets then rapidly transfer to PtOEP where they intersystem cross to the PtOEP triplet state. Since the energy of the CBP triplet state is approximately 0.7 eV higher than that of PtOEP,[6] triplets are strongly localized on PtOEP. In Fig. 2, the transient decay of PtOEP deviates from a monoexponential and becomes increasingly curved with increasing pulse intensities, clearly demonstrating an intensity-dependent quenching of PtOEP triplets.

An implicit assumption in Eq. (4) is a uniform concentration of triplets within an exciton formation zone of thickness d. We note that previous work[4] with 8% PtOEP:Alq_3 has demonstrated that 60% of the triplets are transferred to PtOEP within a length of $\sim$140 Å, with the triplet transfer distance depending on the host material and the dopant concentration. In this work we therefore confine the exciton-formation zone to a thickness of only 100 Å using BCP as a barrier to charge and exciton transport. By trapping carriers and excitons within this narrow region it is reasonable to assume a uniform triplet density.

While it has been established that BCP acts as a barrier to hole transport, we must also ensure confinement of electrons on the opposite side of the luminescent layer. In devices employing Alq_3 as a host, (blue) singlet emission is not observed from α-NPD. Furthermore, α-NPD is closely related to TPD, which has a triplet energy approximately 0.3 eV greater than that of Alq_3.[6] Hence, we infer that α-NPD also acts as a barrier to diffusion of excitons from Alq_3. Unfortunately, α-NPD is not an effective barrier to exciton diffusion if the host material in the luminescent region possesses an energy gap wider than Alq_3. For example, significant emission ($\sim$20%) from α-NPD is observed for luminescent layers consisting of CBP and low doping levels ($\sim$1%) of the phosphors PtOEP and $Ir(ppy)_3$. Nevertheless, confinement of the exciton-formation region and elimination of HTL luminescence is achieved by direct charge trapping on higher densities (>4%) of phosphorescent molecules in CBP.

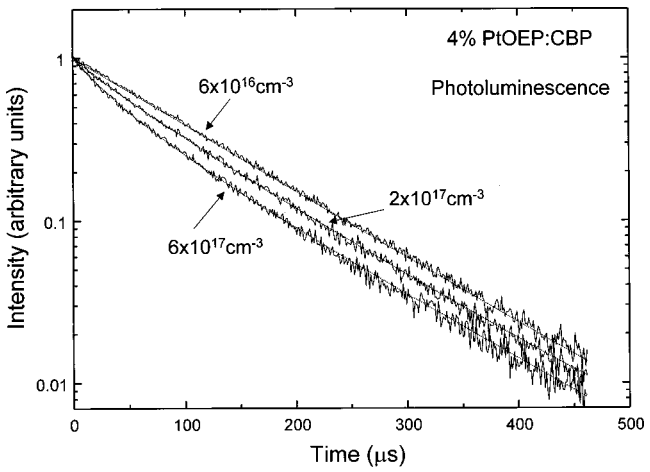

FIG. 2. A selection of transient phosphorescent decays observed after the pulsed photoexcitation of a 4% PtOEP:CBP film. The initial concentrations of PtOEP triplet excitons generated from the pump pulse are also shown. An intensity dependent nonlinearity is observed as the triplet concentration increases. The curves are normalized for comparison.

B. Electroluminescent response of PtOEP doped in CBP ($\Delta G = -0.7$ eV)

The transient response of PtOEP doped into several different host materials was studied as a function of PtOEP concentration and excitation strength. Phosphorescent decay transients were fitted to Eq. (6) to obtain τ and K. The initial concentration of triplets ($[^3M^*(0)]$) was estimated in order to obtain k_{TT} from K [Eq. (7)]. For the electroluminescent (EL) devices, $[^3M^*(0)]$ was determined by integrating the current in the excitation pulse and assuming that charge trapped prior to exciton formation does not significantly contribute to the current. Furthermore, we presume that the exciton-formation efficiency is unity. For the PL studies, $[^3M^*(0)]$ was calculated using an absorption coefficient of $3\times10^5\ cm^{-1}$ for Alq_3[11] and $3\times10^4\ cm^{-1}$ for CBP,[12] both at $\lambda = 337$ nm.

In Fig. 3 we plot the dependence of τ and k_{TT} on $[^3M^*(0)]$ in 8% PtOEP:CBP. Photoluminescence data are shown as squares, and EL data as circles. Within experimental error, both PL and EL data are consistent with $k_{TT} = (3 \pm 1)\times10^{-14}\ cm^3\ s^{-1}$. The lifetime τ, however, varies signifi-

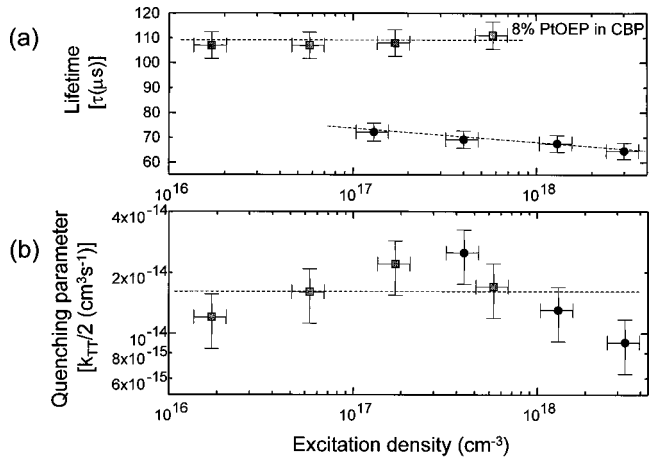

FIG. 3. The lifetime (τ) and biexcitonic quenching rate (k_{TT}) as a function of the initial triplet concentration in 8% PtOEP:CBP. Data points marked by squares and circles are calculated from photoluminescent (PL) and electroluminescent (EL) decays, respectively. As discussed in the text, the significant difference between the PL and EL lifetime of PtOEP is due to absorption by the cathode in the EL structure.

cantly whether measured from the PL or EL data. In Fig. 3(a), the smaller value of τ measured in EL relative to the PL lifetimes is due to nonradiative quenching by the metal cathode in the EL device.[13] Indeed, in agreement with the data, an analytical treatment of radiative lifetimes in optical microcavities[14] predicts that in the structure of Fig. 2, the radiative lifetime should be reduced by 25% relative to its value in the absence of a cathode.

The variation of k_{TT} and τ with PtOEP concentration in a PtOEP:CBP EL device is shown in Fig. 4. The measurements were recorded at a calculated excitation strength of $[{}^3M^*(0)]\sim 1\times 10^{18}\,\mathrm{cm}^{-3}$. As the concentration of PtOEP increases, τ decreases slightly, possibly due to an increase in the number of nonradiative pathways available to triplets in PtOEP aggregates. This is an example of the concentration quenching effect frequently found in fluorescent organic systems.[15] A very weak increase in k_{TT} is also observed as

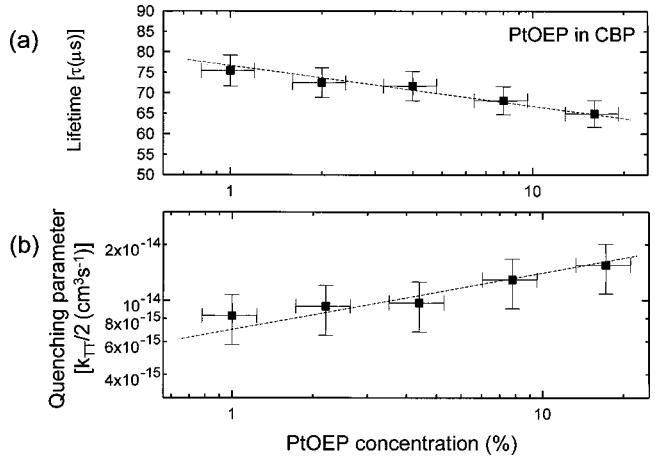

FIG. 4. The lifetime (τ) and biexcitonic quenching rate (k_{TT}) as a function of the concentration of PtOEP in CBP. The data are taken from an electroluminescent device with an initial triplet concentration of $[M^*(0)]\sim 1\times 10^{18}\,\mathrm{cm}^{-3}$.

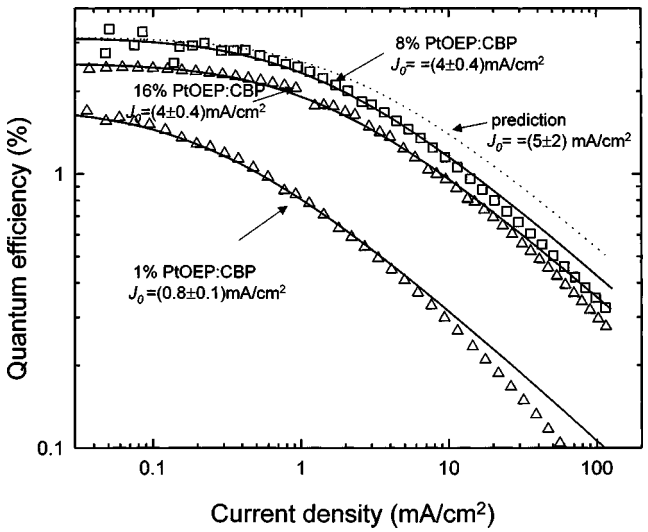

FIG. 5. External quantum efficiency of PtOEP:CBP devices. The solid curves are fits using Eq. (8) and they demonstrate good agreement with the behavior expected for biexcitonic quenching. The only deviation occurs at high current densities ($\sim$100 mA/cm^2) where saturation of PtOEP is important. Parameters extracted from Fig. 3 are used to predict a threshold current for the 8% PtOEP:CBP device of $J_0=5$ mA/cm^2. The best fit to the data (dashed line) yields $J_0=4$ mA/cm^2.

the concentration of PtOEP increases. This results from triplet interactions and T-T annihilation, which increases as triplet percolation between adjacent or clustered PtOEP molecules is enhanced at high doping concentrations.

The external quantum efficiencies of PtOEP:CBP EL devices is shown in Fig. 5. We fit the steady-state characteristics of 1%, 8%, and 16% PtOEP doped in CBP devices to Eq. (8) to determine the value of J_0. The fits are accurate below $J\sim 100\,\mathrm{mA/cm}^2$, where discrepancies occur, a point we shall return to in Sec. VI. Although this demonstrates that the efficiency roll-off observed in PtOEP:CBP devices can be described by Eq. (8), we can also take the parameters extracted from the transient data in Figs. 3 and 4 and directly predict the efficiency characteristics. For example, from the 8% PtOEP:CBP device analyzed in Fig. 3, we obtain $k_{TT}=(3\pm 1)\times 10^{-14}\,\mathrm{cm}^3\,\mathrm{s}^{-1}$ and $\tau=65\pm 5\,\mu$s, yielding a value of $J_0=5\pm 2\,\mathrm{mA\,cm}^{-2}$. This compares well to the observed value of $J_0=4.4\pm 0.4\,\mathrm{mA\,cm}^{-2}$ (see Table I). Thus, nonlinearities in the transient decays of phosphorescent OLED's can be successfully used to predict their steady-state quantum efficiency characteristics. However, the predictions are not nearly as successful for OLED's with low densities of phosphorescent guest molecules. For example, from Fig. 4, we calculate $J_0=7\pm 2\,\mathrm{mA\,cm}^{-2}$ for 1% PtOEP:CBP devices. But fits in Fig. 5 for the same device yield $J_0=0.8\pm 0.1\,\mathrm{mA\,cm}^{-2}$. This apparent discrepancy is also discussed further in Sec. VI.

C. Electroluminescent response of PtOEP:Alq$_3$ ($\Delta G\sim -0.1$ eV)

Similar experiments were performed using PtOEP doped into Alq$_3$. There are several significant differences between

TABLE I. Current densities at the onset of T-T annihilation (J_0) as compared to predictions based on transient decays, and the estimated current density required to saturate the phosphors.

	1% PtOEP in CBP	1% PtOEP in Alq_3	8% PtOEP in CBP	8% PtOEP in Alq_3	16% PtOEP in CBP	16% PtOEP in Alq_3
J_0 from steady-state response (mA/cm^2)	0.8 ± 0.1	2.4 ± 0.2	4.4 ± 0.4	3.8 ± 0.4	4.4 ± 0.4	7.4 ± 0.7
J_0 from transient response (mA/cm^2)	7 ± 2	8 ± 3	5 ± 2	5 ± 2	4 ± 1	6 ± 2
Saturation threshold current density (mA/cm^2)	40 ± 20	200 ± 100	400 ± 80	800 ± 200	800 ± 200	1000 ± 300

these devices and the electroluminescent behavior of PtOEP doped in CBP. In Fig. 6, we observe that the curvature of the PtOEP decay is increased relative to PtOEP:CBP devices shown in Fig. 2. Indeed, in contrast to PtOEP:CBP, even as $[^3M^*(0)]\rightarrow 0$, the PtOEP:Alq_3 system luminescence never approaches a monoexponential decay transient. This curvature may reflect energy transfer processes within the PtOEP:Alq_3 system not included in Eq. (4), or observed in PtOEP:CBP. However, the PtOEP:Alq_3 transient decay still possesses a pronounced intensity dependence; thus the accuracy in the determination of k_{TT} in Fig. 7 improves as $[^3M^*(0)]$ increases. Therefore, measurements of τ and k_{TT} were taken at large values of $[^3M^*(0)]$ ($\sim 1\times10^{18}\,cm^{-3}$). The quenching parameters for EL excitation of a 6% PtOEP:Alq_3 film are $k_{TT}=(1.2\pm0.4)\times10^{-13}\,cm^3\,s^{-1}$ and $\tau=32\pm2\ \mu s$.

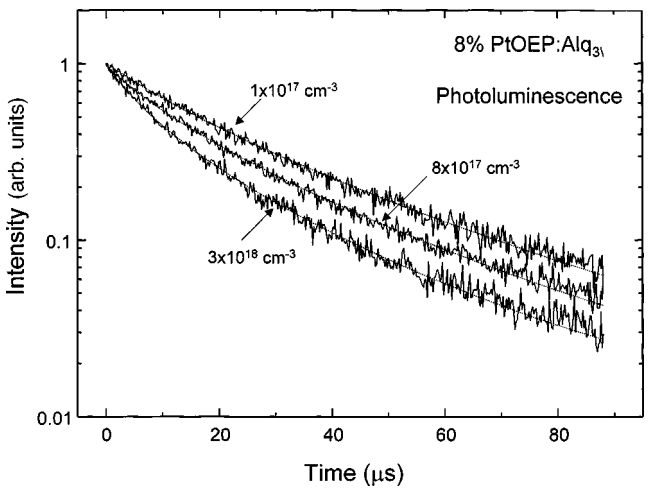

FIG. 6. A selection of transient phosphorescent decays observed after the pulsed photoexcitation of an 8% PtOEP:Alq_3 film. The initial concentrations of PtOEP triplet excitons generated by the pump pulse are indicated. An intensity-dependent nonlinearity is observed as the triplet concentration increases. However, significant intensity-independent curvature is observed in the decay of the weakly excited film. The curves are normalized for comparison.

The twofold decrease in τ for 6% PtOEP:Alq_3 (where $\tau=32\pm2\ \mu s$) relative to 6% PtOEP: CBP $\tau=65\pm5\ \mu s$ is evidence for increased quenching of PtOEP triplets in Alq_3. But it is in the variation of τ and k_{TT} with PtOEP concentration where PtOEP:Alq_3 deviates most significantly from the behavior exhibited by PtOEP:CBP (see Fig. 8). As the concentration of PtOEP increases, τ also increases, opposite to expectations of concentration-induced quenching. Moreover, T-T annihilation as reflected in k_{TT} is found to *decrease* as the concentration of PtOEP increases. Both of these concentration effects and the decrease in τ with decreased PtOEP concentration are manifestations of poor triplet confinement on PtOEP given an energy barrier of only $\Delta G\sim0.1$ eV.[6] As discussed in Sec. VI, the analysis of Eq. (4) is only accurate when triplets are well confined.

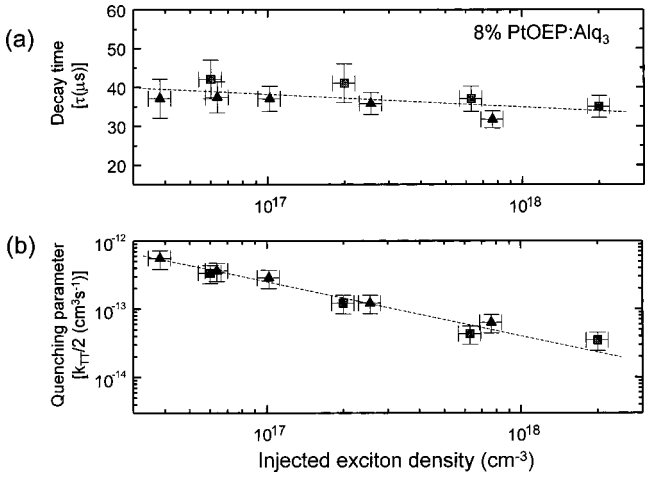

FIG. 7. The lifetime (τ) and biexcitonic quenching rate (k_{TT}) as a function of the initial triplet concentration in 8% PtOEP:Alq_3. Data points marked by squares and triangles are calculated from photoluminescent (PL) and electroluminescent (EL) decays, respectively. Note that the lifetime of PtOEP in Alq_3 is significantly shorter than its lifetime in CBP. Interactions between PtOEP and Alq_3 are responsible for both the reduction in lifetime and the intensity-independent curvature observed in the transient decay of PtOEP in Alq_3.

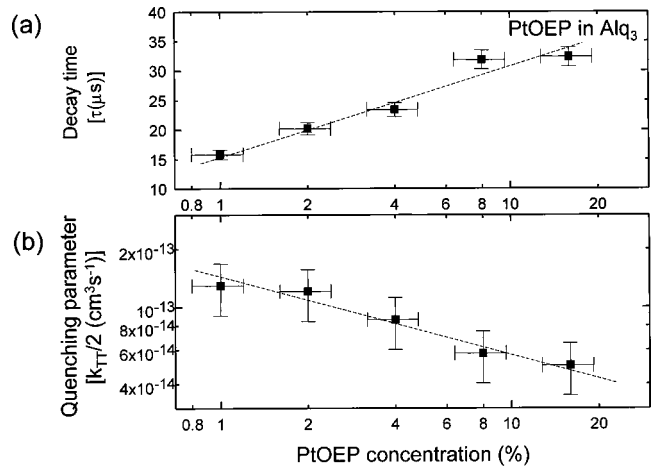

FIG. 8. The lifetime (τ) and biexcitonic quenching rate (k_{TT}) as a function of the concentration of PtOEP in Alq_3. The data are from an electroluminescent device with a high initial triplet concentration of $[M^*(0)]\sim 1\times 10^{18}\,\mathrm{cm}^{-3}$ to minimize errors in the fit due to intensity-independent curvature in the transient decays. Note that contrary to expectations of concentration quenching, the lifetime of PtOEP increases with concentration. This is another example of the importance of PtOEP-Alq_3 interactions in this material system.

The quantum efficiency of PtOEP:Alq_3 nevertheless accurately fits the biexcitonic theory of Eq. (4). As shown in Fig. 9, the predicted quantum efficiency from the transient decay of a 8% PtOEP:Alq_3 device closely matches the steady-state data, although deviations from the theory are again observed at the highest current densities ($\sim$100 mA/cm^2). The results are summarized in Table I, and we observe that the agreement is excellent with the exception of devices with low concentrations of phosphorescent molecules. For example,

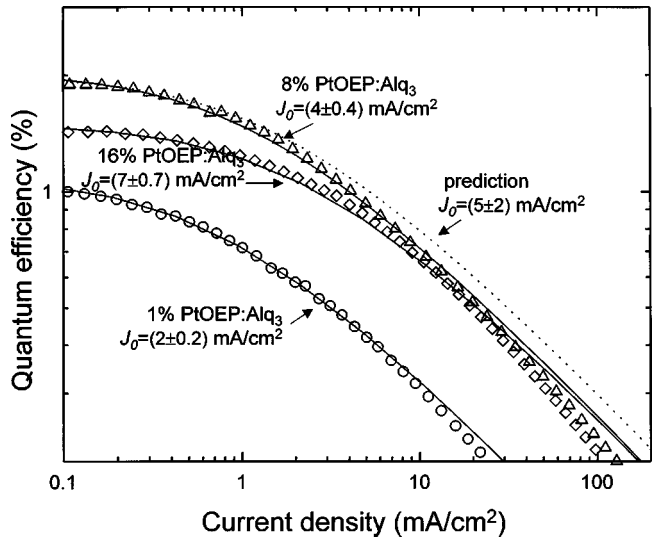

FIG. 9. External quantum efficiency of PtOEP:Alq_3 devices. The solid curves are fits to the data using Eq. (8) and demonstrate good agreement with behavior expected for biexcitonic quenching. The only deviation occurs at high current densities ($\sim$100 mA/cm^2) where saturation of PtOEP is first apparent. Transient parameters plotted in Fig. 7 are used to predict a threshold current for the 8% PtOEP:CBP device of $J_0=5$ mA/cm^2. The best fit to the data (dashed curve) yields $J_0=4$ mA/cm^2.

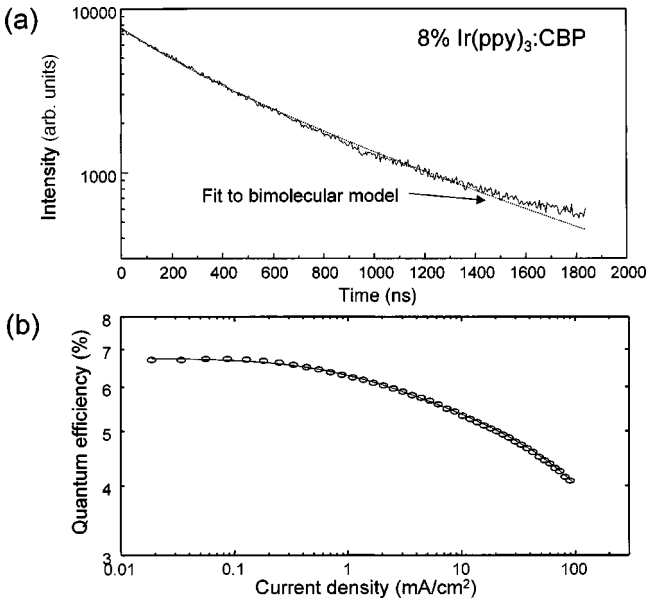

FIG. 10. The transient electroluminescent decay of an 8% $Ir(ppy)_3$:CBP device. The decay cannot be accurately fitted to the theory of Eq. (4), but as discussed in the text, it is possible to fit the transient with a biexponential decay. This behavior is similar to that of PtOEP:Alq_3, and since both of these materials systems possess overlap between guest and host triplet energies, we assume that the intensity-independent curvature observed in $Ir(ppy)_3$:CBP is due to $Ir(ppy)_3$-CBP interactions. Furthermore, we find that the quantum efficiency of $Ir(ppy)_3$:CBP cannot be fitted by a single value of J_0. The quantum efficiency trend can, however, be fit (solid curve) with two values of J_0 ($J_{01}=5.7\,\mathrm{mA/cm^2}, J_{02}=630\,\mathrm{mA/cm^2}$). The fit is obtained by weighting the threshold current densities to 32% J_{01} and 68% J_{02}.

for 8% PtOEP:Alq_3, we calculate $J_0=5\pm 2\,\mathrm{mA\,cm^{-2}}$ from the transient data and measure $J_0=3.8\pm 0.4\,\mathrm{mA\,cm^{-2}}$ from the steady-state efficiency data.

D. Electroluminescent response of $Ir(ppy)_3$ in CBP ($\Delta G=-0.2$ eV)

The intensity-independent curvature found in PtOEP:Alq_3 is also observed in $Ir(ppy)_3$:CBP devices, but in this case the effect is so strong that the transients cannot be fitted to the model of Eq. (4). This is apparent in Fig. 10, where we show the transient response of a 6% $Ir(ppy)_3$:CBP EL device for $[^3M^*(0)]\sim 1\times 10^{18}\,\mathrm{cm}^{-3}$. The $Ir(ppy)_3$ transient exhibits at least two characteristic decay times, and a biexponential fit yields $\tau_1\sim 400$ ns and $\tau_2\sim 1300$ ns. We note that without a firm physical basis for this behavior there is no clear justification for performing a biexponential fit to the data, as it is extremely difficult to distinguish a biexponential fit from a more complex distribution of transient lifetimes.[16] However, we take the $Ir(ppy)_3$ transient curvature as evidence of additional processes in $Ir(ppy)_3$:CBP unaccounted for in the theory of Eq. (4). As in the case of PtOEP and Alq_3, we note that these additional processes appear to be related to the small energy difference ($\Delta G=-0.2$ eV) between triplet energies of the host and guest.[6] Thus, it is likely that in both PtOEP:Alq_3 and $Ir(ppy)_3$:CBP, T-T annihilation is present in both the host and guest, and that energy transfer between

the two species is responsible for the multiple lifetimes needed to model the transient decays. By accounting for triplet-host interactions, these processes are modeled in Sec. VI. However, triplets in the host are undetectable in our luminescent experiments, and their behavior remains unquantified.

Given that it is not possible to accurately fit the $Ir(ppy)_3$:CBP transient decays with a single value of τ and k_{TT}, it follows that the quantum efficiency of $Ir(ppy)_3$:CBP must also be fit by more than a single value of J_0. In Fig. 10, we show that the quantum efficiency trend can be fitted with two values of J_0 ($J_{01}=5.7\,mA/cm^2$, $J_{02}=630\,mA/cm^2$). Due to the square dependence of onset current density on lifetime this range is plausible. The fit is obtained by weighting the onset current densities as 32% J_{01} and 68% J_{02}. Despite doubts over the exact mechanism, the efficiency roll-off exhibited by $Ir(ppy)_3$:CBP nevertheless indicates that these devices are similarly dominated by biexcitonic quenching.

E. Electroluminescent response of PtOEP:Ir(ppy)$_3$ ($\Delta G=-0.5$ eV, $k_F=10^7\,s^{-1}$)

The previous examples have all employed fluorescent donors; however, systems featuring a phosphorescent donor are also of interest because of the possibility for Förster energy transfer from the triplet state of the donor to the singlet state of the acceptor. Indeed, this mechanism has already been successfully used to transfer triplet states to a fluorescent dye and thereby increase its electroluminescent efficiency.[10] The process is relatively fast and occurs over a long range ($\sim$40 Å) if the dipoles on the participating species are strongly coupled. Hence it may be possible to use phosphorescent host materials to simultaneously minimize host triplet lifetimes and the concentration of phosphorescent guests. Both of these effects should act to reduce triplet interactions, thereby reducing the importance of T-T annihilation.

To test this concept, we employed $Ir(ppy)_3$ as a host material for PtOEP. Similar to PtOEP in Alq_3, there is strong overlap between the emission of $Ir(ppy)_3$ and the absorption of PtOEP, ensuring the energetic resonance needed to facilitate transfer. Using the structure of Fig. 1(a), we fabricated two devices with emissive layers of 1% PtOEP in either CBP or $Ir(ppy)_3$. The quantum efficiency of both devices is shown in Fig. 11. Evidently, using $Ir(ppy)_3$ as a host material not only increases the overall quantum efficiency of PtOEP emission, but also increases the T-T annihilation onset current to $J_0=7\,mA/cm^2$ from $J_0=0.8\,mA/cm^2$. Since the phosphorescent lifetime of PtOEP is similar in both cases ($\sim$70 μs), the PL efficiency of PtOEP is unchanged. The energy confinement of triplets is also similar for PtOEP:CBP and PtOEP:$Ir(ppy)_3$; thus the difference in the strength of T-T annihilation in these two cases suggests that the rate of energy transfer may be slower for PtOEP:CBP, resulting in a higher proportion of mobile host triplets in the latter material combination. These host triplets participate readily in T-T annihilation, lowering both J_0 and the maximum quantum efficiency. Triplet transfer in PtOEP:CBP is dependent on the concentration of PtOEP, but at least at these low densities ($\sim$1%), the results indicate that triplet transfer from CBP to PtOEP is slower than $10^7\,s^{-1}$. The successful doping of PtOEP into $Ir(ppy)_3$ reflects a possible mechanism for improving the performance of phosphorescent OLED's.

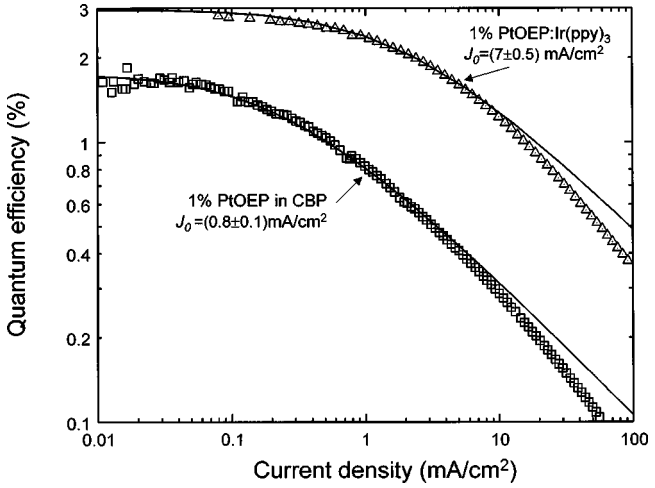

FIG. 11. The external quantum efficiencies of a 1% PtOEP:$Ir(ppy)_3$ device in comparison to a 1% PtOEP:CBP device. It is expected that significant Förster energy transfer occurs from the triplet state of $Ir(ppy)_3$ to PtOEP, minimizing the triplet lifetime in the host. This may be responsible for the significantly increased onset current (J_0) of T-T annihilation observed in the $Ir(ppy)_3$-based devices. Note that the emission spectrum contains $Ir(ppy)_3$ as well as PtOEP phosphorescence, but the quantum efficiency shown is that of PtOEP emission only.

F. Electroluminescent response of Eu(TTA)$_3$phen:CBP

The triplet-triplet annihilation model can also be applied to rare-earth complexes. Similar to PtOEP and $Ir(ppy)_3$, excitons in the ligands of these well-studied[17,18] complexes efficiently cross intersystem from singlets to triplets. In $Eu(TTA)_3$phen (see inset, Fig. 12), triplets on the TTA ligands are then transferred to the central ion, exciting a ^5D_x state of Eu^{3+}. Spectrally sharp phosphorescence at 612 nm with a decay lifetime of $\sim$300 μs results from the Eu^{3+} $^5D_0 \rightarrow {}^7F_2$ transition.[12]

Unlike the other phosphors studied in this work, the phosphorescent decay of the Eu^{3+} ion is monoexponential and independent of the initial excitation density (see Fig. 12). However, in Fig. 13 we find that the steady-state bimolecular T-T annihilation model of Eq. (8) fits the measured EL quantum efficiency of a 2% $Eu(TTA)_3$phen:CBP device. The onset of T-T annihilation is observed at $J_0=6\pm1\,mA/cm^2$, but the intensity-independent decay [Fig. 12(b)] of $Eu(TTA)_3$phen phosphorescence demonstrates that the quenching observed must occur *prior* to energy transfer to the Eu^{3+} ion. The TTA triplet has a lifetime of only $\sim$0.1 μs;[12] thus in the absence of an additional triplet state, TTA triplets are not expected to be present in sufficient densities to cause significant T-T annihilation. Analysis[12] of the donor and acceptor energy levels reveals that triplet energy transfer from CBP to TTA is relatively weak, and consequently CBP triplets exist in high densities, promoting guest-host triplet annihilation. In Sec. V, we eliminate the possibility of charge-carrier–triplet annihilation. Thus, given the good fits to Eq. (8), we must conclude that T-T annihilation exerts a

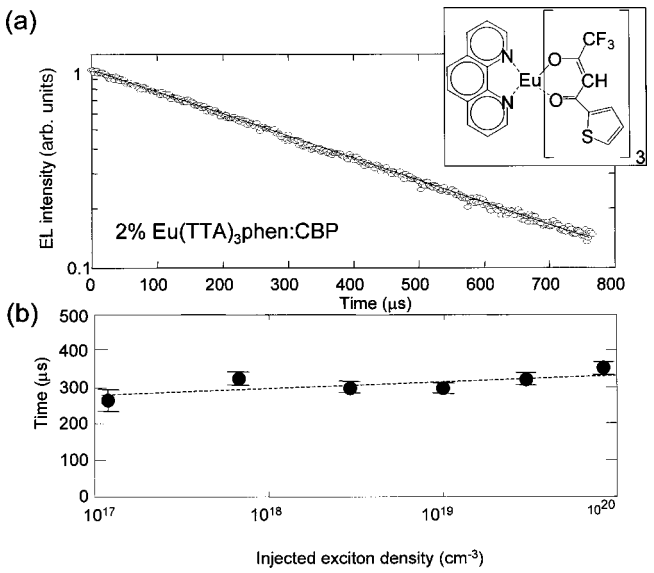

FIG. 12. (a) The electroluminescent decay of 2% $Eu(TTA)_3phen$ in CBP given an injected exciton density of $\sim 8\times 10^{19}\,cm^{-3}$. The decay is monoexponential, demonstrating that Eu^{3+} excited states do not participate in bimolecular T-T quenching. The structure of the device was ITO/TPD/$Eu(TTA)_3$phen:CBP/BCP/Alq_3/MgAg (Ref. 12). Inset: The chemical structure of $Eu(TTA)_3phen$. (b) The characteristic phosphorescent lifetime as a function of current density.

significant effect on all systems where triplet excitons possess $\sim$1-μs lifetimes and participate in energy transfer.

V. TRIPLET-POLARON ANNIHILATION

An alternative model for quenching is triplet-polaron annihilation.[7,12] On examination, however, this model not only fails to explain the quenching observed in the photoluminescence of PtOEP:CBP, it also does not yield a quadratic dependence of annihilation on excitation density. For example, if we assume that the concentration of steady-state space or trapped charge far exceeds the concentration of free charge, then this annihilation process follows:[7,12]

$$\frac{d[^3M^*]}{dt} = -\frac{[^3M^*]}{\tau} - k_e[^3M^*][n_t] + \frac{J}{qd}, \qquad (11)$$

where k_e is the polaron-triplet annihilation rate in the active region, and $[n_t]$ is the average concentration of trapped charge. Assuming bulk limited transport,[19,20] then $[n_t]$ is proportional[21] to the applied potential V, and we can solve Eq. (11) in steady state to get

$$\frac{\eta}{\eta_0} = \frac{1}{1+\alpha V}, \qquad (12)$$

where α is a constant. We find that in our devices $J \propto V^{l+1}$, with $l \sim 8$. Hence, Eq. (12) can never possess the form of Eq. (8) and cannot be made to fit the observed trends in quantum efficiency (see Fig. 13).

However, if transport is not bulk limited and $[n_t]$ is not proportional to the applied potential V, then $J \propto [n_t]^{l+1}$, where $l > 0$. If $l = 1$, corresponding to space-charge-limited transport, then Eq. (12) has the same form as Eq. (8) and can be made to fit the observed trends in quantum efficiency (see Fig. 13). In order to test the significance of polaron-triplet quenching it is necessary to measure its magnitude. This was performed by observing changes in the transient decay of PtOEP molecules in the presence of an electron current in an Alq_3 host. The structure employed consisted of a 1000-Å-thick Alq_3 film deposited on indium tin oxide (ITO), the center 100 Å was doped with 6% PtOEP, and a Mg:Ag cathode was deposited as in the EL devices discussed earlier. When a dc bias was applied, poor hole injection from ITO ensured dominantly electron current in the film. Ultraviolet laser pulses were applied through the ITO substrate, and the decay of the PtOEP molecules was measured on a streak camera. The transient response as a function of current density is shown in Fig. 14(a), with fits to Eq. (5). Changes in both the linear and nonlinear terms were observed, possibly indicating the quenching of both Alq_3 and PtOEP triplets at different rates. But in order to assess the rate of polaron–PtOEP-triplet annihilation, only the linear component of the decay was studied.

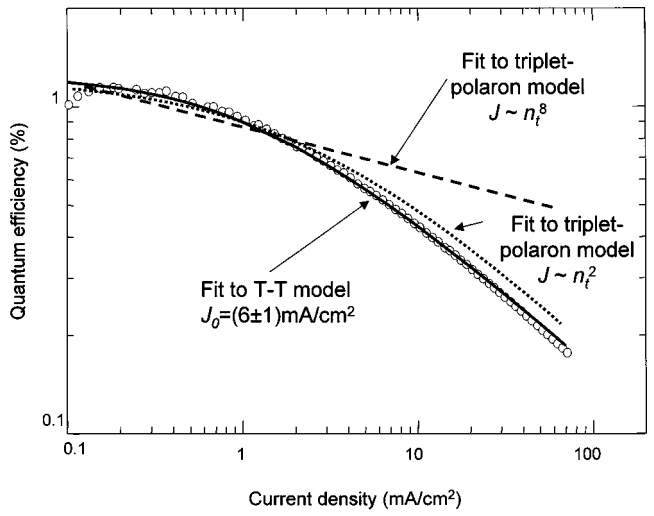

FIG. 13. The external quantum efficiency of the $Eu(TTA)_3$phen:CBP device. It exhibits a roll-off characteristic of T-T annihilation with an onset current density of $J_0 = 6 \pm 1\,mA\,cm^{-2}$. The expected behavior of polaron-triplet quenching for bulk-limited transport ($J \propto [n_t]^8$) does not fit the data. However, good agreement is obtained for polaron-triplet quenching models where $J \propto [n_t]^2$.

The linear component (τ) decreased with increasing current density; however, the quenching was observed to be much weaker than the T-T effects studied earlier. The lifetime was reduced to half its initial value at a current density of $J_0 = 200\,mA\,cm^{-2}$ [see Fig. 14(b)], over two orders of magnitude greater than the onset current densities for T-T annihilation. We also note that electric-field-induced luminescence quenching[22] is indistinguishable from polaron-triplet annihilation in this experiment. Although the field varies only slightly from $1\times 10^6\,V\,cm^{-1}$ at $J = 13\,mA\,cm^{-2}$ to $1.3\times 10^6\,V\,cm^{-1}$ at $J = 255\,mA\,cm^{-2}$. In any case, the magnitude of the observed quenching is much less than T-T effects and can be ignored in most electrophosphorescent devices.

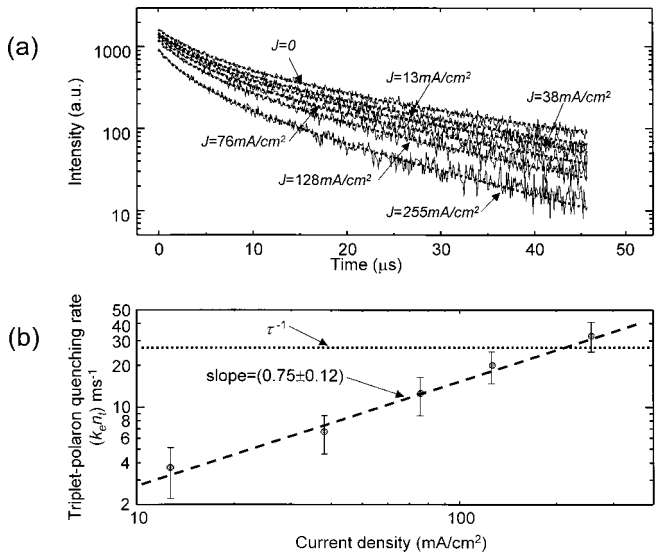

FIG. 14. (a) PtOEP transient decays observed after pulsed photoexcitation of a 6% PtOEP:Alq_3 film. The doped region is 100 Å thick and contained within a 1000-Å-thick film of Alq_3. Electrical bias was applied to generate electron current and examine the effect of triplet-polaron quenching. (b) The measured polaron-triplet quenching rate compared to the measured lifetime of PtOEP emission in the absence of current. The current density where the efficiency of emission falls to half its initial value is $J_0 = 170\ \mathrm{mA\ cm^{-2}}$.

VI. DISCUSSION

The measured and predicted values of J_0 are shown in Table I for a range of PtOEP concentrations in both CBP and Alq_3. For comparison, the saturation current density thresholds were also calculated using Eq. (10). Good agreement is observed between the theoretical predictions of T-T annihilation effects and the quantum efficiency of highly doped PtOEP devices.

However, the predictions of simple T-T annihilation following Eq. (4) fail for low concentrations of PtOEP. For low concentrations of guest molecules, emission from Alq_3 or α-NPD in the case of CBP-based devices, is typically responsible for >20% of the total emission. Thus, it is difficult to calculate $[^3M^*(0)]$ and hence k_{TT} from Eq. (7). Overestimating $[^3M^*(0)]$ by ignoring the fraction of excitons in the host or HTL artificially depresses k_{TT}, leading to an overestimate of J_0.

It is likely that the density of host triplets will be highest for devices with low concentrations of phosphorescent acceptors. Discrepancies between steady-state and transient data should therefore arise due to the neglect of host triplets in the theory of Eq. (4). It remains for us to evaluate the assumption that only guest triplets participate in the annihilation process.

If we assume that the guest phosphorescent molecules are distributed throughout the host, then even at high triplet densities of $\sim 10^{18}\ \mathrm{cm^{-3}}$, the average spacing between guest excited states is ~100 Å. But triplet transfer requires significant overlap of the molecular orbitals of the donor and acceptor molecules, and since overlap is an exponential function of separation, we would expect that k_{TT} should increase with increasing triplet density. However, this was not observed, as indicated in Sec. IV. Neither is it possible for triplets to percolate between guest molecules, and aggregates in excess of 10^4 molecules are required to account for the observation of T-T annihilation at excitation densities as low as $10^{16}\ \mathrm{cm^{-3}}$. Therefore, we conclude that host triplets are responsible for the quenching of guest triplets. For systems where triplets are not tightly bound to guest molecules such as $Ir(ppy)_3$:CBP or PtOEP:Alq_3, triplets can diffuse from guest to host. However, for PtOEP:CBP or TPD the energy difference between host and guest is as high as 0.7 eV.

We have already demonstrated that triplet transfer in 2% PtOEP:CBP is slower than $10^7\ \mathrm{s^{-1}}$. The energy transfer has two components: triplet diffusion in CBP and then transfer from PtOEP to CBP. By increasing the doping concentration of PtOEP in CBP, the triplet diffusion times can be reduced, but even at 8–16% PtOEP:CBP, T-T annihilation is still observed, indicating the existence of mobile host triplets. Thus, we conclude that the large energy difference between the triplet levels of PtOEP and CBP results in inversion of the transfer rate. From Eq. (2) in Paper I, if we assume a typical[23] energy barrier of $\lambda \sim 0.1$ eV and calculate k_F for CBP to PtOEP ($\Delta G = -0.7$ eV) we find that Marcus transfer is in the inverted region. Although the value of λ is unknown for these materials, it seems plausible that triplets persist in the host because the energy difference is such that k_F is small.

Given the presence of host triplets we must reassess the accuracy of Eqs. (4) and (8). In steady state, it is easy to show from Eq. (1) in Paper I that if triplets are primarily formed on the guest as is the case with PtOEP in CBP, then

$$[^3M_H^*] = \frac{k_R}{k_F + k_H}[^3M_G^*], \tag{13}$$

or, if triplets are formed on the host, then

$$[^3M_H^*] = \frac{k_R + k_G}{k_F}[^3M_G^*]. \tag{14}$$

Here, subscripts G and H correspond to guest and host, respectively. Similarly, k_G and k_H are the decay rates of triplets on the guest and host, respectively. Equation (1) in Paper I contains only linear terms and does not consider bimolecular annihilation. Thus, for steady-state excitation, while T-T annihilation is small, the guest and host triplet concentrations are in equilibrium and Eq. (8) is accurate. This is reflected in the curve fits in Figs. 5, 9, and 11, which break down as T-T annihilation becomes stronger. Given Eqs. (13) and (14), in this case the triplet annihilation rate in Eq. (4) should be replaced by

$$k_{TT}^* = k_{TT}\frac{k_R}{k_F + k_H} \quad \text{or} \quad k_{TT}^* = k_{TT}\frac{k_R + k_G}{k_F}. \tag{15}$$

Equation (4) is valid for transient decays if equilibrium is maintained between host and guest triplet populations, i.e., $[^3M_H^*] \propto [^3M_G^*]$. This requires that $k_R \gg k_G$ and $k_F \gg k_H$. However, given the relatively rapid rates of triplet decay in PtOEP and $Ir(ppy)_3$, and the sometimes large energy barrier between guest and host, it is unlikely that the first condition is true. Thus, for transient analysis, Eq. (4) should be rewritten to include all the possible triplet interactions, guest-host (k_{GH}), host-host (k_{HH}), and guest-guest (k_{GG}), i.e.,

$$\begin{aligned}\frac{d[^3M_H^*]}{dt} &= -k_H[^3M_H^*] + k_R[^3M_G^*] - \tfrac{1}{2}k_{GH}[^3M_G^*][^3M_H^*] \\ &\quad - \tfrac{1}{2}k_{HH}[^3M_H^*]^2, \\ \frac{d[^3M_G^*]}{dt} &= -k_G[^3M_G^*] + k_F[^3M_H^*] - \tfrac{1}{2}k_{GH}[^3M_G^*][^3M_H^*] \\ &\quad - \tfrac{1}{2}k_{GG}[^3M_G^*]^2.\end{aligned} \tag{16}$$

Unfortunately, in the absence of knowledge of the host triplet population, the additional parameters in Eq. (16) make analysis of transient data more difficult. But we can neglect guest-guest T-T annihilation (e.g., $k_{GG} \sim 0$) because the guest triplets are well separated. Relative to host-guest interactions, host-host T-T annihilation ($k_{HH}[^3M_H^*]^2 \sim 0$) can also be neglected since the host triplet concentration is likely to be significantly smaller than the guest triplet concentration. At low concentrations of guest molecules the host triplet density increases and this later assumption breaks down, leading to the discrepancies we observe for low concentrations of phosphorescent guests. However, applying both these assumptions, we are left with linear terms and the same bimolecular term in both equations. In the limit of large guest triplet densities, the decays of both host and guest triplets are dominated by this guest-host annihilation term. Only in this limit does Eq. (4) become similar to Eq. (16). Hence the transient analysis of Eq. (4) is correct only in the limit of large triplet densities.

VII. CONCLUSION

The quantum efficiency roll-off is arguably the most significant problem facing electrophosphorescent devices. By demonstrating a link between nonlinearities in the transient behavior and steady-state quantum efficiency, T-T annihilation is identified as the principal cause of this roll-off. The strength of the annihilation process is linked to the likelihood of interaction between triplet states. In particular, the phosphorescent lifetime and the concentration of phosphorescent sites determine the current at the onset of T-T annihilation. Efforts to improve the efficiency of electrophosphorescent emission should therefore concentrate on minimizing the lifetime of triplet states and obtaining rapid energy transfer of triplets to low concentrations of phosphorescent sites. Short lifetime phosphors such as $Ir(ppy)_3$ have considerably reduced T-T effects, and lanthanide complexes may also deserve further investigation due to the short lifetime of the triplet state participating in energy transfer to the rare-earth-metal phosphorescent ion. However, both materials require hosts with an energetic triplet state to encourage triplet transfer.

This work has also provided evidence that annihilation of host triplets is a significant loss mechanism in many systems. To counter this effect, it is possible to employ a phosphorescent host that participates in long-range and rapid Förster energy transfer to a guest. This not only reduces the lifetime of host triplets but also enables improved energy transfer at low guest concentrations. Indeed, experiments demonstrating energy transfer from $Ir(ppy)_3$ to a fluorescent guest[10] and $Ir(ppy)_3$ to PtOEP have demonstrated that there is significant potential in such approaches.

ACKNOWLEDGMENTS

This work was funded by Universal Display Corporation, the Defense Advanced Research Projects Agency, the Air Force Office of Scientific Research, and the National Science Foundation MRSEC program.

[1] M. A. Baldo, D. F. O'Brien, Y. You, A. Shoustikov, S. Sibley, M. E. Thompson, and S. R. Forrest, Nature (London) **395**, 151 (1998).

[2] D. F. O'Brien, M. A. Baldo, M. E. Thompson, and S. R. Forrest, Appl. Phys. Lett. **74**, 442 (1999).

[3] M. A. Baldo, S. Lamansky, P. E. Burrows, M. E. Thompson, and S. R. Forrest, Appl. Phys. Lett. **75**, 4 (1999).

[4] M. A. Baldo, D. F. O'Brien, M. E. Thompson, and S. R. Forrest, Phys. Rev. B **60**, 14 422 (1999).

[5] V. Cleave, G. Yahioglu, P. Le Barny, R. Friend, and N. Tessler, Adv. Mater. **11**, 285 (1999).

[6] M. A. Baldo and S. R. Forrest, preceding paper, Phys. Rev. B 62, 10 958 (2000).

[7] M. Pope and C. Swenberg, *Electronic Processes in Organic Crystals* (Oxford University Press, Oxford, 1982).

[8] N. J. Turro, *Modern Molecular Photochemistry* (University Science Books, Mill Valley, 1991).

[9] I. G. Hill and A. Kahn, J. Appl. Phys. **86**, 4515 (1999).

[10] M. A. Baldo, M. E. Thompson, and S. R. Forrest, Nature (London) **403**, 750 (2000).

[11] D. Z. Garbuzov, V. Bulovic, P. E. Burrows, and S. R. Forrest, Chem. Phys. Lett. **249**, 433 (1996).

[12] C. Adachi, M. A. Baldo, and S. R. Forrest (unpublished).

[13] V. Bulovic, V. B. Khalfin, G. Gu, P. E. Burrows, D. Z. Garbuzov, and S. R. Forrest, Phys. Rev. B **58**, 3730 (1998).

[14] From Fig. 2 in Bulović *et al.* (Ref. 13), and given our OLED structure, we have $(W_{tot} - W_{NR})/W_0 \sim 2$, where W_{tot} is the total recombination rate of an exciton in the microcavity, W_{NR} is the nonradiative rate minimally affected by the cavity, and W_0 is the intrinsic radiative rate. Now for PtOEP in Alq_3, $\eta_{PL} = W_0/(W_0 + W_{NR}) \sim \frac{1}{3}$, where η_{PL} is the photoluminescent efficiency of PtOEP in Alq_3 (Ref. 11). Since $\eta_{EL} = W_0/W_{tot}$, solving the equations we get $\eta_{EL}/\eta_{PL} = \frac{3}{4}$.

[15] C. W. Tang, S. A. VanSlyke, and C. H. Chen, J. Appl. Phys. **65**, 3610 (1989).

[16] D. R. James and W. R. Ware, Chem. Phys. Lett. **120**, 455 (1985).

[17] J. Kido, K. Nagai, Y. Okamoto, and T. Skotheim, Chem. Lett. **1991**, 1267.
[18] J. Kido, H. Hayese, K. Hongawa, K. Nagai, and K. Okuyama, Appl. Phys. Lett. **65**, 2124 (1994).
[19] P. E. Burrows, Z. Shen, V. Bulovic, D. M. McCarty, S. R. Forrest, J. A. Cronin, and M. E. Thompson, J. Appl. Phys. **79**, 7991 (1996).
[20] A. J. Campbell, M. S. Weaver, D. G. Lidzey, and D. D. C. Bradley, J. Appl. Phys. **84**, 6737 (1998).
[21] M. A. Lampert and P. Mark, *Current Injection in Solids* (Academic, New York, 1970).
[22] W. Stampor, J. Kalinowski, P. D. Marco, and V. Fattori, Appl. Phys. Lett. **70**, 1935 (1997).
[23] G. L. Closs and J. R. Miller, Science **240**, 440 (1988).